Scheme 1. Dirhenium−Benzamidinate Compounds[a]

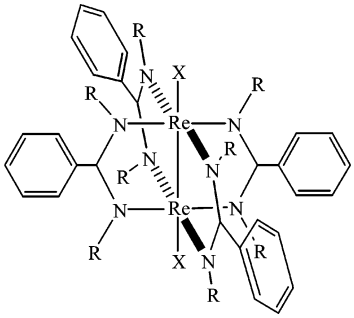

[a] **1**, R = CH_3, X = Cl; **2**, R = C_2H_5, X = Cl; **3**, R = CH_3, X = NO_3.

nium tetraformamidinate complex was reported recently.[11] Many diruthenium compounds supported by *N*,*N*′-dialkylbenzamidinates have been synthesized during the last three years,[12] revealing the potential of amidinate ligands in supporting dinuclear species. Described in this contribution are the synthesis and spectroscopic and structural characterization of dirhenium paddlewheel compounds supported by *N*,*N*′-dialkylbenzamidinate ligands (Scheme 1).

Results and Discussion

Synthesis. Earlier preparation of $Re_2(DMBA)_4Cl_2$ (**1**) was based on the molten reaction between $(Bu_4N)_2[Re_2Cl_8]$ and HDMBA (*N*,*N*′-dimethylbenzamidine), and the yield of **1** was not established due to the existence of the byproduct $Re_2(DMBA)_2Cl_4$.[13] The combination of using $Re_2(OAc)_4Cl_2$ as the Re_2 starting material and an extended reaction time resulted in compound **1** as the sole product in excellent yield. $Re_2(DEBA)_4Cl_2$ (**2**) was obtained similarly with the replacement of HDMBA with HDEBA (*N*,*N*′-diethylbenzamidine). $Re_2(DMBA)_4(NO_3)_2$ (**3**) was obtained from the reaction between $Re_2(DMBA)_4Cl_2$ and $AgNO_3$ in a CH_2Cl_2/CH_3CN solution. Similarly, the reaction between $Re_2(DMBA)_4Cl_2$ and $AgBF_4$ also led to the removal of both axial chloro ligands.[14] Previously, treating Re_2(di(*p*-MeOphenyl)formamidinate)$_4Cl_2$ with 2 equiv of $AgBF_4$ only resulted in the loss of one of two axial chloro ligands.[15] The difference in reactivity may be attributed to the fact that DMBA is a much stronger donor than formamidinate, which increases electron density on the Re_2 core and reduces its affinity to the axial chloro ligands.

Molecular Structures. The structures of compounds **1**−**3** have been established through single crystal X-ray diffraction studies, and their structural plots are shown in Figures 1−3, respectively. The crystal structure of **1** with CCl_4 as the lattice solvent was previously determined in the space group *I*4/*mmm*,[13] while the crystal structure of **1** in the current study

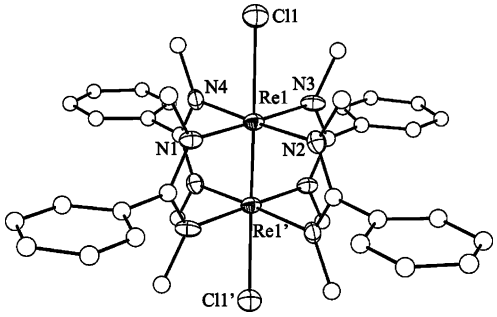

Figure 1. ORTEP plot of $Re_2(DMBA)_4Cl_2$ at 30% probability level. Hydrogen atoms were omitted for clarity.

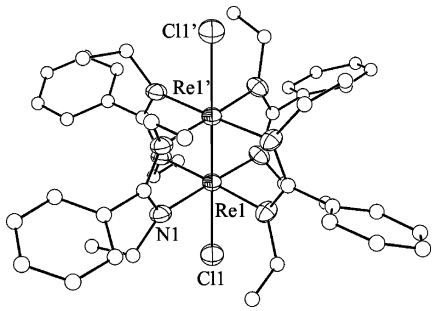

Figure 2. ORTEP plot of $Re_2(DEBA)_4Cl_2$ at 30% probability level. Hydrogen atoms and the water solvent molecule were omitted for clarity.

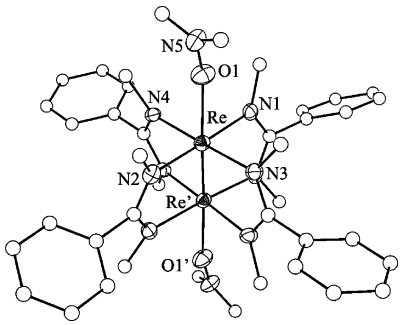

Figure 3. ORTEP plot of $Re_2(DMBA)_4(NO_3)_2$ at 30% probability level. Hydrogen atoms were omitted for clarity.

contains no lattice solvent and is of low symmetry. Interestingly, compound **2** crystallizes in the same space group *I*422 as $Ru_2(DEBA)_4Cl_2$ even though the latter has no interstitial solvent.[12c] Crystals of both compound **3** and $Ru_2(DMBA)_4(NO_3)_2$,[12b] having the same space group and nearly identical unit cells, are isomorphous.

All three compounds exhibit the expected paddlewheel topology. As shown in Table 1, the Re−Re bond lengths of $Re_2(DMBA)_4Cl_2$ and $Re_2(DEBA)_4Cl_2$ are 2.2120(9) and 2.2168(6) Å, respectively, which are comparable to those of the previously characterized $Re_2(DMBA)_4Cl_2$ (2.208(2) Å)[13] and $Re_2(hpp)_4Cl_2$ (2.191(1) Å),[16] and slightly shorter than those of $Re_2(DArF)_4Cl_2$ (2.232−2.284 Å).[17] These bond lengths are all within the range expected for compounds with a Re−Re quadruple bond.[2] Similar to most of the aforementioned Re_2 species, both compounds exhibit a very small

(11) Bradley, P. M.; Smith, L. T.; Eglin, J. L.; Turro, C. *Inorg. Chem.* **2003**, *42*, 7360.
(12) (a) Xu, G.-L.; Campana, C.; Ren, T. *Inorg. Chem.* **2002**, *41*, 3521. (b) Xu, G.-L.; Jablonski, C. G.; Ren, T. *Inorg. Chim. Acta* **2003**, *343*, 387. (c) Xu, G.-L.; Jablonski, C. G.; Ren, T. *J. Organomet. Chem.* **2003**, *683*, 388. (d) Hurst, S. K.; Xu, G.-L.; Ren, T. *Organometallics* **2003**, *22*, 4118. (e) Chen, W.-Z.; Ren, T. *Inorg. Chem.* **2003**, *42*, 8847. (f) Xu, G.-L.; DeRosa, M. C.; Crutchley, R. J.; Ren, T. *J. Am. Chem. Soc.* **2004**, *126*, 3728.
(13) Cotton, F. A.; Ilsley, W. H.; Kaim, W. *Inorg. Chem.* **1980**, *19*, 2360.
(14) Dequeant, M. Q.; Ren, T. Unpublished results.
(15) Barclay, T.; Eglin, J. L.; Smith, L. T. *Polyhedron* **2001**, *20*, 767.
(16) Cotton, F. A.; Gu, J. D.; Murillo, C. A.; Timmons, D. J. *J. Chem. Soc., Dalton Trans.* **1999**, 3741.
(17) (a) Cotton, F. A.; Ren, T. *J. Am. Chem. Soc.* **1992**, *114*, 2495. (b) Eglin, J. L.; Lin, C.; Ren, T.; Smith, L.; Staples, R. J.; Wipf, D. O. *Eur. J. Inorg. Chem.* **1999**, 2095.

N−Re−Re′−N′ twist (0.7° for **1** and 3.4° for **2**). Compounds **1** and **2** have identical Re−Cl bond lengths (2.637 Å), which are significantly shorter than that of $Re_2(hpp)_4Cl_2$ (2.749 Å), but much longer than those of $Re_2(DArF)_4Cl_2$ (2.49−2.53 Å). The variation in Re−Cl bond lengths is consistent with the known donor ability of *N*,*N*′-bidentate bridging ligands:[18] the stronger the donor, the longer the axial Re−Cl bond.

Table 1. Selected Bond Lengths (Å) and Angles (deg) for Compounds **1**−**3**

	1	2	3
Re(1)−Re(1)′	2.2120(9)	2.2168(6)	2.1731(5)
Re(1)−N(1)	2.065(11)	2.099(5)	2.090(6)
Re(1)−N(2)	2.079(10)		2.055(6)
Re(1)−N(3)	2.077(11)		2.095(6)
Re(1)−N(4)	2.104(10)		2.086(6)
Re(1)−Cl(1)	2.637(4)	2.637(3)	
Re(1)−O(1)			2.345(6)
N(1)−Re(1)−N(2)	89.5(4)	89.979(4)	90.9(2)
N(1)−Re(1)−N(3)	177.7(4)	177.82(19)	176.7(2)
N(1)−Re(1)−N(4)	90.6(4)	89.979(4)	89.9(2)
N(1)−Re(1)−Re(1)′	91.0(3)	91.09(9)	91.18(17)
N(1)−Re(1)−Cl(1)	89.5(3)	88.91(9)	
Re(1)′−Re(1)−Cl(1)	178.21(8)	180.0	
N(1)−Re(1)−O(1)			85.9(2)
Re(1)′−Re(1)−O(1)			177.12(16)
N−Re−Re′−N′ (averaged)	0.7	3.4	7.1

In carrying out the anion metathesis reaction between $Re_2(DMBA)_4Cl_2$ and $AgNO_3$, we anticipated the incorporation of solvent molecules such as CH_3CN at both axial positions of the Re_2 core. Hence it was a surprise that the structural study revealed the axial ligation by NO_3^- (Figure 3). Compound **3** displays both a long axial Re−O bond (2.345(6) Å) and a 0.04 Å decrease in Re−Re bond length in comparison with the parent compound **1**. Clearly, the weak σ-donor nitrate has a minimal interaction with the Re d_{z^2} orbital, which results in an enhancement of the Re−Re σ-bond relative to the chloro compound.

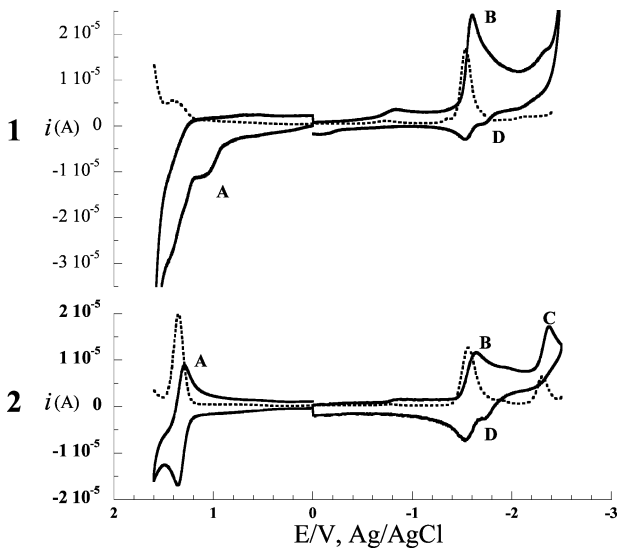

Figure 4. Cyclic voltammograms (—) and differential pulse voltammograms (···) of compounds **1** and **2** recorded in THF.

Electrochemistry. Both the cyclic and differential pulse voltammograms (CV and DPV) were recorded for compounds **1** and **2** (Figure 4), while those of compound **3** were not obtained, due to a solubility problem. The CV of compound **2** shows a quasireversible oxidation at 1.33 V (A), a quasireversible reduction at −1.57 V (B), and an irreversible reduction at −2.37 V (C). The quasireversibility of both A and B couples permits an estimation of the HOMO−LUMO gap of the solvated Re_2-species as follows: $E_g = E_{1/2}(A) - E_{1/2}(B) = 2.90$ V.[19] The observed couples are likely all Re_2-based, and a tentative assignment is given in Scheme 2. Both the appearance of couple D and the irreversibility of couple C are attributed to the dissociation of axial chloro ligand(s) upon reductions. Similar behavior due to the dissociation of axial ligands has been frequently observed in diruthenium−amidinate compounds.[12] It is clear from the CV of **1** that the redox stability of the Re_2 species is greatly reduced with DMBA as the bridging ligand: all couples are irreversible, and the second reduction (C) is not detected at all, indicating a complete disintegration of the dirhenium species upon the first reduction.

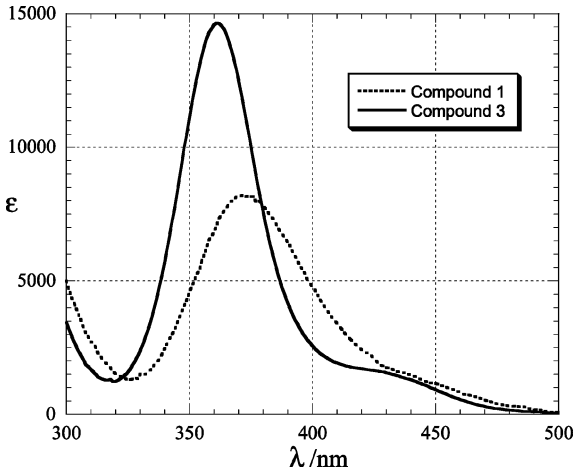

Figure 5. Visible spectra of compounds **1** and **3** recorded in CH_2Cl_2.

Scheme 2. Redox Steps and Related Chemical Steps in $Re_2L_4Cl_2$

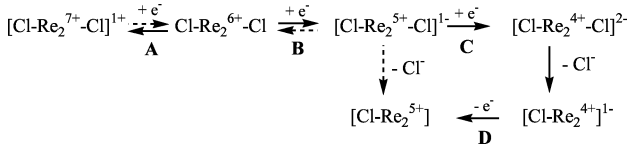

Photophysical Properties. The electronic absorption spectra of compounds **1** and **3** are shown in Figure 5, while the absorption, emission, and excitation spectra of **2** are shown in Figure 6. Compounds **1** and **2** feature an intense absorption at 372 and 369 nm (ca. 3.3 eV), respectively, and a shoulder at ca. 440 nm ($E = 2.8$ eV). Upon substitution of the axial chloro ligands with nitrate, both the intense peak and the shoulder in **3** are blue shifted relative to that of **1**, and are observed at 361 and 430 nm, respectively. In previous studies of related species, the $\delta \rightarrow \delta^*$ transition was assigned to the peak at 368 nm in $Re_2(DPhF)_4Cl_2$,[16] and the peak at 360 nm in $Re_2(hpp)_4Cl_2$.[16] By analogy to these systems, it

(18) Ren, T.; Parrish, D. A.; Deschamps, J. R.; Eglin, J. L.; Xu, G.-L.; Chen, W.-Z.; Moore, M. H.; Schull, T. L.; Pollack, S. K.; Shashidhar, R.; Sattelberger, A. P. *Inorg. Chim. Acta* **2004**, *357*, 1313.
(19) Ren, T. *Coord. Chem. Rev.* **1998**, *175*, 43.

would be logical to attribute the intense peak at around 370 nm in **1**−**3** to the $\delta \rightarrow \delta^*$ transition. However, compelling spectroscopic evidence and the energetics derived from a two-state model presented here suggests that the shoulder at ~440 nm is a better candidate for this transition. In addition, the transition energy of the shoulder at 2.8 eV matches well with the HOMO−LUMO gap derived from the CV of **2** (2.90 eV).

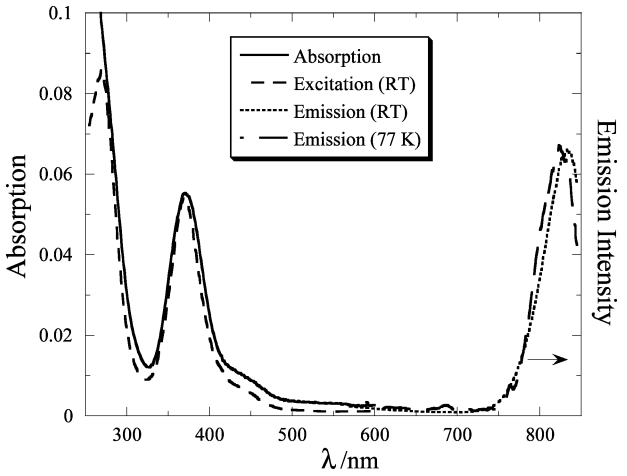

Figure 6. Electronic absorption, emission ($\lambda_{exc} = 370$ nm), and excitation ($\lambda_{em} = 830$ nm) spectra of CH_2Cl_2 solutions of **2** at room temperature and emission from the solid ($\lambda_{exc} = 370$ nm) at 77 K.

Upon excitation of CH_2Cl_2 solutions of **2** with 350−450 nm light at room temperature, emission was observed with the maximum at 833 nm (Figure 6). The excitation spectrum of **2** at room temperature in CH_2Cl_2 ($\lambda_{em} = 830$ nm) exhibits good overlap with the absorption of the compound under similar experimental conditions (Figure 6), indicating that the emission arises from the dirhenium compound. As shown in Figure 6, a slight blue shift of 10 nm (130 cm^{-1}) of the luminescence maximum of **2** is observed in the solid at 77 K with respect to the solution spectrum, which is typical for the $^1\delta\delta^*$ emission of quadruply bonded complexes, such as $Mo_2Cl_4(PBu_3)_4$.[5] Similar solution emission is observed for **1**, and its solid state spectrum at 77 K exhibits a vibronic progression with $\Delta\nu_{av} = 272$ cm^{-1}, a value close to those previously reported for the Re−Re stretch of the related $Re_2(O_2CR)_4Cl_2$ complexes.[2] These results point at a strong coupling of the electronic transition giving rise to the emission along the Re−Re quadruple bond stretch coordinate, consistent with the luminescence arising from a $\delta\delta^*$ excited state.

The Stokes shifts of the $^1\delta\delta^*$ absorption and emission of Mo_2, W_2, and Re_2 complexes usually range from 2000 to 3000 cm^{-1}.[2,5−10] However, the Stokes shift observed for the emission of **1** and **2** is ca. 14 900 cm^{-1} (Figure 6), and is similar to that recently reported for the $^3\delta\delta^*$ emission from $Re_2(DpAniF)_4Cl_2$ (DpAniF is di(4-methoxyphenyl)formamidinate).[11] Since theoretical calculations and experiments agree that the $^3\delta\delta^*$ excited state of quadruply bonded bimetallic complexes lies at ~10 000 cm^{-1} below the $^1\delta\delta^*$ state,[20−23] it is possible that the luminescence from **1** and **2** arises from the $^3\delta\delta^*$ excited state of the molecules.

The emission of **2** is relatively independent of solvent polarity, with maxima at 830, 831, 833, and 829 nm in toluene, dichloromethane, acetone, and acetonitrile, respectively. Similar insensitivity to the solvent was previously reported for the $^1\delta\delta^*$ emission of various quadruply bonded complexes.[5,24] The lack of solvent dependence is consistent with the luminescence arising from a metal-centered state, such as $^3\delta\delta^*$, rather than a charge transfer state involving the amidinate ligands. The large Stokes shift of the emission, along with its insensitivity to solvent polarity and ν(Re−Re) vibronic progression, lends support to the conclusion that the luminescence arises from the $^3\delta\delta^*$ excited state of the molecule.

The energies of the $^1\delta\delta^*$ and $^3\delta\delta^*$ excited electronic states can be estimated from the one-electron energy difference between the δ and δ^* levels, ΔW, and the electron exchange, K, and are given by eqs 1 and 2.[21−23]

$$E(^1\delta\delta^*) = [(\Delta W)^2 + K^2\,]^{1/2} + \mathrm{K} \qquad (1)$$

$$E(^3\delta\delta^*) = [(\Delta W)^2 + K^2\,]^{1/2} - \mathrm{K} \qquad (2)$$

The energies of the $^1\delta\delta^*$ and $^3\delta\delta^*$ excited states and the value of ΔW are sensitive to both the torsional angle (overlap of the d_{xy} orbitals), χ,[20] and the energies of the δ and δ^* orbitals, which in turn depend on their mixing with linear combinations of orbitals from the bridging ligands.[22b] Given that the value of K is relatively invariant to the ligand system, an average of the values reported or calculated by us for nine different Re_2(III,III) complexes, 5080 cm^{-1}, was used here.[22b,25] Assuming that the emission of **2** arises from the $^3\delta\delta^*$ of the molecule, eq 2 can be used to determine $\Delta W =$ 18 117 cm^{-1} with $E(^3\delta\delta^*) =$ 13 736 cm^{-1}. Utilizing these values of K and ΔW, eq 1 results in $E(^1\delta\delta^*) =$ 23 863 cm^{-1} (419 nm). This energy for the $^1\delta\delta^*$ overlaps better with the shoulder observed at 440 nm than with the strong peak at ~360 nm.

The remaining issue is the origin of the peak at ca. 370 nm in **1** and **2**. DFT calculations of both $Re_2(hpp)_4Cl_2$ and the model compound $Re_2(HNC(H)NH)_4Cl_2$ and detailed analysis were presented earlier by Cotton et al.[16] Because of the nearly eclipsed geometry of compounds **1**−**3**, the MO scheme derived for $Re_2(HNC(H)NH)_4Cl_2$ is relevant and used as a qualitative guide here. Clearly, the $\delta(b_{2g}) \rightarrow \delta^*(b_{1u})$ transition is allowed by parity. The other possible excitations accessible in near-UV and visible regions include $\delta(b_{2g}) \rightarrow$

(20) (a) Cotton, F. A.; Eglin, J. L.; Hong, B.; James, C. A. *J. Am. Chem. Soc.* **1992**, *112*, 4915. (b) Cotton, F. A.; Eglin, J. L.; Hong, B.; James, C. A. *Inorg. Chem.* **1993**, *32*, 2104.
(21) (a) Bursten, B. E.; Cotton, F. A.; Fanwick, P. E.; Stanley, G. G. *J. Am. Chem. Soc.* **1983**, *105*, 3082. (b) Bursten, B. E.; Clark, D. L. *Polyhedron* **1987**, *6*, 695.
(22) (a) Hopkins, M. D.; Zietlow, T. C.; Miskowski, V. M.; Gray, H. B. *J. Am. Chem. Soc.* **1985**, *107*, 510. (b) Hopkins, M. D.; Gray, H. B.; Miskowski, V. M. *Polyhedron* **1987**, *6*, 705.
(23) (a) Hay, P. J. *J. Am. Chem. Soc.* **1978**, *100*, 2897. (b) Hay, P. J. *J. Am. Chem. Soc.* **1982**, *104*, 7007.
(24) Cotton, F. A.; Curtis, N. F.; Johnson, B. F. G.; Robinson, W. R. *Inorg. Chem.* **1965**, *4*, 326.
(25) (a) Ebner, J. R.; Walton, R. A. *Inorg. Chem.* **1975**, *14*, 1987. (b) Srinivasan, V.; Walton, R. A. *Inorg. Chem.* **1980**, *19*, 1635. (c) Dunbar, K. R.; Walton, R. A. *Inorg. Chem.* **1985**, *24*, 5.

$\pi^*(e_g)$, $\sigma(Re-Cl)(a_{1g}) \rightarrow \pi^*(e_g)$, and $\sigma(Re-Cl)(a_{1g}) \rightarrow \delta^*(b_{1u})$. The first two are clearly forbidden by parity, but the latter is allowed and hence may be responsible for the absorption at 370 nm. The substantial Cl contribution to the $\sigma(Re-Cl)$ orbital provides charge transfer character to this transition, which explains its high intensity.

Conclusion

Structural and spectroscopic studies of new Re_2−amidinate compounds revealed both similarities to and subtle differences from the previously studied dirhenium compounds $Re_2(DArF)_4Cl_2$ and $Re_2(hpp)_4Cl_2$. Unique to the amidinate compounds is the ability to form an axial nitrato complex, which may provide the access to axial alkynyl compounds using the conditions developed for the analogous diruthenium compounds.[12] The unusual observation of $^3\delta\delta^*$ phosphorescence from these complexes is noteworthy.

Experimental Section

$AgNO_3$ was purchased from Baker Analytical, and all solvents were purchased from VWR. $Re_2(OAc)_4Cl_2$,[24] *N*,*N*′-dimethylbenzamidine (HDMBA),[26] and *N*,*N*′-diethylbenzamidine (HDEBA)[26] were prepared as previously described. ^{1}H NMR spectra were recorded on a Bruker AVANCE300 NMR spectrometer, with chemical shifts (δ) referenced to the residual solvent $CDCl_3$. Electronic absorption spectra in CH_2Cl_2 were obtained on either a Perkin-Elmer Lambda-900 UV−vis−NIR spectrophotometer or a Hewlett-Packard diode array spectrometer (HP 8453). Emission spectra were collected on a SPEX FluoroMax-2 spectrometer equipped with a 150 W xenon source, a red-sensitive R928P photomultiplier tube, and DataMax-Std software on a desktop computer. Cyclic and differential pulse voltammograms were recorded in 0.2 M *n*-Bu_4NPF_6 solution (THF, N_2-degassed) on a CHI620A voltammetric analyzer with a glassy carbon working electrode (diameter = 2 mm), a Pt-wire auxiliary electrode, and a Ag/AgCl reference electrode. The concentration of dirhenium species is always 1.0 mM.

Synthesis of $Re_2(DMBA)_4Cl_2$ (1). $Re_2(OAc)_4Cl_2$ (0.100 g, 0.147 mmol) and *N*,*N*′-dimethylbenzamidine (HDMBA) (0.87 g, 5.9 mmol) were placed in a 50 mL Schlenk tube fitted with a coldfinger and heated in a sand bath at 140°C for 36 h under argon. During this time, the mixture changed from a coral color to a dark orange. Once cooled, 10 mL of ethyl acetate was added to the mixture, and the slurry was filtered. The orange filtrate contains mostly the unreacted ligand and unidentified byproducts. The yellow solid collected was identified as $Re_2(DMBA)_4Cl_2$, which was recrystallized from CH_2Cl_2 to yield yellow plate crystals (0.12 g, 79%). MS-FAB (*m*/*e*, based on ^{186}Re): 996 [$(Re_2(DMBA)_4Cl)^+$]. ^{1}H NMR: 7.60 (m), 7.31 (d), 3.38 (s). Anal. Calcd for $C_{36}H_{44}N_8Cl_2Re_2$: C, 41.89, H, 4.31, N, 10.86. Found: C, 41.68, H, 4.30, N, 10.63. Electrochemical data: E_{pa}(A), 1.08 V; $E_{1/2}$(B), −1.563 V (ΔE_p, 0.078 V; $i_{backward}/i_{forward}$, 0.28). UV−vis, λ_{max}, nm (ϵ, M^{-1} cm^{-1}): 372 (8220).

Synthesis of $Re_2(DEBA)_4Cl_2$ (2). $Re_2(OAc)_4Cl_2$ (0.100 g, 0.147 mmol) and *N*,*N*′-diethylbenzamidine (HDEBA) (1.30 g, 7.35 mmol) were placed in a 50 mL Schlenk tube fitted with a coldfinger and heated to a molten state in a sand bath at 125 °C for 96 h under argon. Upon cooling, the reaction mixture was extracted with 20 mL of hexane in order to remove excess ligand and byproducts. The solid collected was dissolved in CH_2Cl_2 and filtered. The filtrate was concentrated to ca. 2 mL and layered with 30 mL of hexanes. $Re_2(DEBA)_4Cl_2$ was collected as dark orange square pyramidal crystals (0.096 g, 57%) after 4 days. MS-FAB (*m*/*e*, based on ^{186}Re): 1072 [$(Re_2(DEBA)_4Cl)^+$]. Anal. Calcd for $C_{44}H_{60}N_8Cl_2Re_2$: C, 45.46, H, 5.39, N, 9.64. Found: C, 45.44, H, 5.14, N, 9.82. Electrochemical data, $E_{1/2}$/V, ΔE_p/V, $i_{backward}/i_{forward}$: A, 1.327, 0.071, 0.66; B, −1.586, 0.111, 0.50; E_{pc}(C), −2.37 V. UV−vis, λ_{max}, nm (ϵ, M^{-1} cm^{-1}): 369 (9940) and ca. 450.

Table 2. Crystal Data and Structural Refinement

	1	**2**·4H_2O	**3**
chemical formula	$C_{36}H_{44}N_8Cl_2Re_2$	$C_{44}H_{68}Cl_2N_8O_4Re_2$	$C_{36}H_{44}N_{10}O_6Re_2$
fw	1032.09	1216.36	1085.21
space group	*P*1̄	*I*422	*Pbcn*
a, Å	9.5810(9)	14.4466(8)	12.3390(9)
b, Å	10.2213(9)	14.4466(8)	21.0758(15)
c, Å	11.618(1)	12.0711(9)	15.4168(11)
α, deg	104.589(2)		
β, deg	113.628(2)		
γ, deg	102.727(2)		
V, Å^3	940.2(2)	2519.3(3)	4009.2(5)
Z	1	2	4
T, °C	27	27	27
λ(M*o* Kα), Å	0.71073	0.71073	0.71073
ρ_{calc}, g/cm^3	1.823	1.593	1.798
μ, mm^{-1}	6.611	4.953	6.089
R	0.064	0.030	0.029
wR2	0.160	0.086	0.060

Synthesis of $Re_2(DMBA)_4(NO_3)_2$ (3). $Re_2(DMBA)_4Cl_2$ (0.050 g, 0.048 mmol) was dissolved in 15 mL of CH_2Cl_2, to which was added $AgNO_3$ (0.16 g in 15 mL of MeCN) dropwise. The resultant solution was stirred under argon for 24 h, and the AgCl precipitate was filtered off. Upon the solvent removal from the filtrate, the residue was first dissolved in 20 mL of acetonitrile and filtered in order to get off any starting material, and then dissolved in 20 mL of CH_2Cl_2 in order to get off excess $AgNO_3$. $Re_2(DMBA)_4(NO_3)_2$ was crystallized from the CH_2Cl_2 extract as red-orange plates (0.043 g, 82%). MS-FAB (*m*/*e*, based on ^{186}Re): 978 [$(Re_2(DMBA)_4)^{2+}$-(H_2O)]. ^{1}H NMR: 7.68 (m), 7.60(m), 7.37 (m), 3.15 (s). Anal. Calcd for $C_{36}H_{44}N_{10}O_6Cl_2Re_2$·$2H_2O$: C, 38.56, H, 4.32, N, 12.49. Found: C, 38.59, H, 4.08, N, 12.48. UV−vis, λ_{max}, nm (ϵ, M^{-1} cm^{-1}): 361 (14 650) and ca. 430.

Structure Determination. Single crystals were obtained as previously stated. X-ray intensity data were measured at 300 K on a Bruker SMART1000 CCD-based X-ray diffractometer system using Mo Kα (λ = 0.71073 Å). Crystals used for data collection were cemented to a quartz fiber with epoxy glue. Data were measured using ω scans of 0.3° per frame for 5 s for **1**, and 10 s for both **2** and **3** so that a hemisphere (1271 frames) was collected. The frames were integrated with the Bruker SAINT software package[27] using a narrow-frame integration algorithm, which also corrects for the Lorentz and polarization effects. Absorption corrections were applied using SADABS.

Structures were solved and refined using the Bruker SHELXTL (version 5.1) software package[28−30] in space groups of *P*1̄ (**1**), *I*422 (**2**), and *Pbcn* (**3**). Positions of all non-hydrogen atoms were revealed by a direct method. All non-hydrogen atoms are anisotropic, and the hydrogen atoms were put in calculated position and

(26) Bradley, W.; Wright, I. *J. Chem. Soc.* **1956**, 640.

(27) *SAINT V 6.035 Software for the CCD Detector System*; Bruker-AXS Inc.: Madison, WI, 1999.

(28) *SHELXTL 5.03 (WINDOW-NT Version), Program Library for Structure Solution and Molecular Graphics*; Bruker-AXS Inc.: Madison, WI, 1998.

(29) Sheldrick, G. M. *SHELXS-90, Program for the Solution of Crystal Structures*; University of Göttingen: Göttingen, Germany, 1990.

(30) Sheldrick, G. M. *SHELXL-93, Program for the Refinement of Crystal Structures*; University of Göttingen: Göttingen, Germany, 1993.

riding mode. Each structure was refined to convergence by least-squares method on F^2, SHELXL-93, incorporated in SHELXTL.PC V 5.03. Selected bond lengths and angles are provided in Table 1, and crystallographic data are given in Table 2.

Acknowledgment. This work was supported in part by the National Science Foundation (CHE0242623 to T.R.), the Office of Naval Research (N00014-03-1-0531 to T.R.), the University of Miami (CCD diffractometer fund), and the National Institutes of Health (RO1 GM64040-01 to C.T.).

The authors wish to dedicate this contribution to Professor Richard A. Walton on the occasion of his 65th birthday in recognition of his paramount contribution to rhenium chemistry.

Supporting Information Available: X-ray crystallographic files in CIF format for the structure determination of compounds **1**−**3**. This material is available free of charge via the Internet at http://pubs.acs.org.

IC0487981